Preparation and Magnetic Properties of AlN/Phenolic Resin-Coated Iron-Based Soft Magnetic Composites

Shen Wu[1] · Zhenzhen Dong[1] · Jiechao Li[1] · Jianglei Fan[1] · Yachao Liang[2] · Jianxiu Liu[1]

Abstract

Soft magnetic composites (SMCs) were prepared by uniformly mixing reduced Fe powder with nano-AlN particles and phenolic resin by powder metallurgy. The effects of AlN content on the microstructure, density and magnetic properties of iron-based soft magnetic composites were investigated. Scanning electron microscopy (SEM) and energy-dispersive spectroscopy (EDS) analysis showed that the sample prepared with AlN/phenolic resin insulation has a thin and uniform coating layer. Compared with the single inorganic AlN-coated sample, the AlN/phenolic resin composite coating method resulted in increased electrical resistivity and compact density, reducing the eddy current loss and effectively reducing the magnetic loss of the soft magnetic composites. The 4 wt.% AlN/phenolic resin soft magnetic composite had the lowest magnetic loss (147.67 W/kg@100 kHz,0.05 T), which was 90.4% lower than that of a single AlN-coated sample, and the permeability of the sample was stabilized at 90 in a wide range of frequencies.

Introduction

As a magnetic functional material, soft magnetic composites (SMCs) have the advantages of low coercivity and eddy current loss, good frequency characteristics and three-dimensional isotropy, and they are widely used in automotive electronics, computers, home appliances, mobile communications and other fields.[1–3] In recent years, SMCs have been rapidly developed, and with their application in high-performance semiconductors and the increasing demand for energy-efficient solutions, reducing magnetic loss in SMCs has become a priority. The magnetic core loss of SMCs generally includes hysteresis loss, eddy current loss and residual loss. Within its applicable scope, eddy current loss is the main loss form,[4] which is usually reduced by coating insulating materials on the surface of the magnetic matrix. The coating can improve the resistivity of the material to a certain extent, but also leads to a decrease in the permeability and saturation magnetic flux density of the material. Therefore, the development of suitable insulating coating materials has become a research hotspot for SMCs.

Current insulating materials are mainly divided into two types: inorganic insulating materials and organic insulating materials. For example, SiO_2,[5] Al_2O_3,[6] MgO,[7,8] phosphate[9] and others have good heat resistance and insulation properties, can maintain stability at high temperatures, effectively reduce the influence of internal stress, and improve the resistivity of SMCs to reduce eddy current loss. However, the inorganic material itself is brittle, cannot obtain a large density during pressing, and cannot effectively cover the magnetic matrix, which is not conducive to reducing the magnetic loss of the sample. Common organic coating materials are generally thermosetting resins, such as epoxy resin[10] and phenolic resin,[11] which have the advantages of strong fluidity and excellent mechanical properties. When used as insulation coating materials, they can be uniformly coated on the surface of magnetic matrix, but they are not resistant to high temperature, and the internal stress and dislocation of the sample cannot be eliminated in subsequent heat treatment. As a result, the hysteresis loss of the material will increase, and thus the total loss will increase.[12] Traditional phenolic resin[13] will decompose above 300°C.

✉ Shen Wu
  wszzuli@126.com

1 College of Mechanical and Electrical Engineering, Zhengzhou University of Light Industry, Zhengzhou 450002, China

2 Engineering Division, Huanghe Science and Technology College, Zhengzhou 450063, China

Strečková et al.[14] coated iron powder with SiO_2-modified phenolic resin to prepare soft magnetic composite materials. They found that the complete decomposition temperature of the modified phenolic resin was 70°C higher than that of the unmodified phenolic resin, but it was still not sufficient to effectively eliminate the internal stress generated during pressing.

AlN has good thermal conductivity, with theoretical thermal conductivity of up to 320 W m^{-1} K^{-1}, and has excellent insulation properties usually greater than 10^{14} Ω cm. AlN is not harmful to the environment due to its stable chemical properties,[15–18] and has been widely used in recent years. When used as insulation coating material, it can effectively improve the resistivity of the material and reduce the magnetic loss. Xiaoxi et al.[19] reported in situ generation of an AlN-Al_2O_3 composite insulation layer on the surface of FeSiAl powder through surface nitriding oxidation technology, and the insulation layer and the powder matrix maintained a good interface combination, endowing the material with higher permeability and a higher quality factor. Despite the excellent properties of AlN, however, the problems of high brittleness and poor pressing performance of the material prepared as a coating material have not been overcome, and a single organic coating does not have high-temperature resistance or excellent thermal conductivity. In this experiment, the complementary advantages of AlN and phenolic resin were combined to prepare organic-inorganic composite insulating coating materials, and the effects of different contents of AlN on the microstructure and magnetic properties of soft magnetic composite materials during the inorganic-organic composite coating were studied.

Materials and Methods

Materials

The magnetic matrixes used in this research were irregular reduced iron powders provided by Changsha Tianjiu Metal Materials Co., Ltd., with an average particle size of 75 μm. The AlN particles used as coating material with an average particle size of 40 nm were purchased from Taipeng Metal Materials Co., Ltd. The experimental phenolic resin was supplied by Henan Hengyuan New Materials Co., Ltd., anhydrous ethanol and xylene (analytical grade) were produced by Luoyang Chemical Reagent Factory, glycerol was provided by Xilong Science Co., Ltd., and zinc stearate was obtained from Tianjin Miou Chemical Reagent Co., Ltd.

Experimental Methods

The reduced iron powder (100 g) was washed with anhydrous ethanol and dried and then put into a coupling agent diluent mixed with 5% (volume fraction) KH550 and 95% (volume fraction) anhydrous ethanol for coupling treatment, with a mass ratio of KH550 to Fe powder of 1:100. Meanwhile, the pH of the solution was adjusted to 9, and the solution was stirred for 2 h and then dried in vacuum at 50°C. Then phenolic resin and 1 wt.%, 2 wt.%, 3 wt.%, 4 wt.%, 5 wt.%, and 6 wt.% AlN were added to xylene to prepare different coating suspensions. Next, 100 g of the coupled reduced iron powders was placed in the suspension and stirred for 1 h and dried at 50°C to obtain uniformly coated composite materials. Finally, 0.5 wt.% glycerol and zinc stearate were added to the prepared AlN/phenolic resin soft magnetic composite to increase the internal lubricity of the material. In addition, a single AlN-coated composite (4 wt.%) was prepared using the same method. Under pressure of 600 MPa, the prepared composite material was pressed into annular samples with dimensions of Φ40 mm×Φ32 mm×4 mm, and the stress was removed by heat treatment at 500°C for 1 h in argon atmosphere.

Microscopic Characterization

The surface morphology, microstructure and elemental distribution of Fe powders and SMC samples were examined by electron microscopy (SEM; Phenom XL100) and energy-dispersive spectroscopy (EDS; Phenom XL100). The composition distribution of the coated sample after polishing was characterized via element line scanning. The density of samples was measured by the Archimedes drainage method, and the resistivity of the samples was tested by the four-probe method. The AC magnetic properties of the SMC samples including permeability, magnetic loss and quality factor were measured using a B-H analyzer (SY-8219) at different frequencies when Bm was 50 mT.

Results and Analysis

Characterization of SMCs

Figure 1 shows the morphological characteristics of reduced iron powders in different coating states. It can be seen that, compared with uncoated reduced iron powder, the surface of the iron powder after insulation coating became relatively rough, and there were fine particles attached to the surface, indicating that the surface of the substrate was coated with insulating materials. Compared with Fig. 1a and 1b, the surface adhesion of iron powder in Fig. 1c is more obvious and relatively flat, indicating that the fluidity of phenolic resin in the composite coating material improved the coating effect. Figure 2 shows the distribution of elements of the magnetic powder with different coating agents. It can be seen that, compared with single AlN coating, the surface of
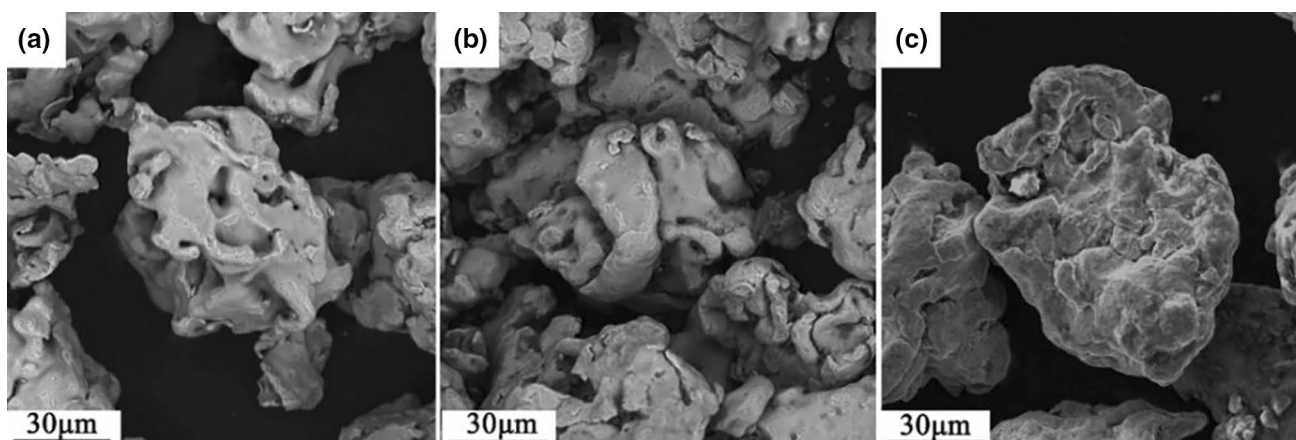
Fig. 1 SEM diagram of magnetic particles: (a) original reduced Fe powder; (b) 4% AlN-coated powder; (c) 4% AlN/phenolic resin-coated powder.
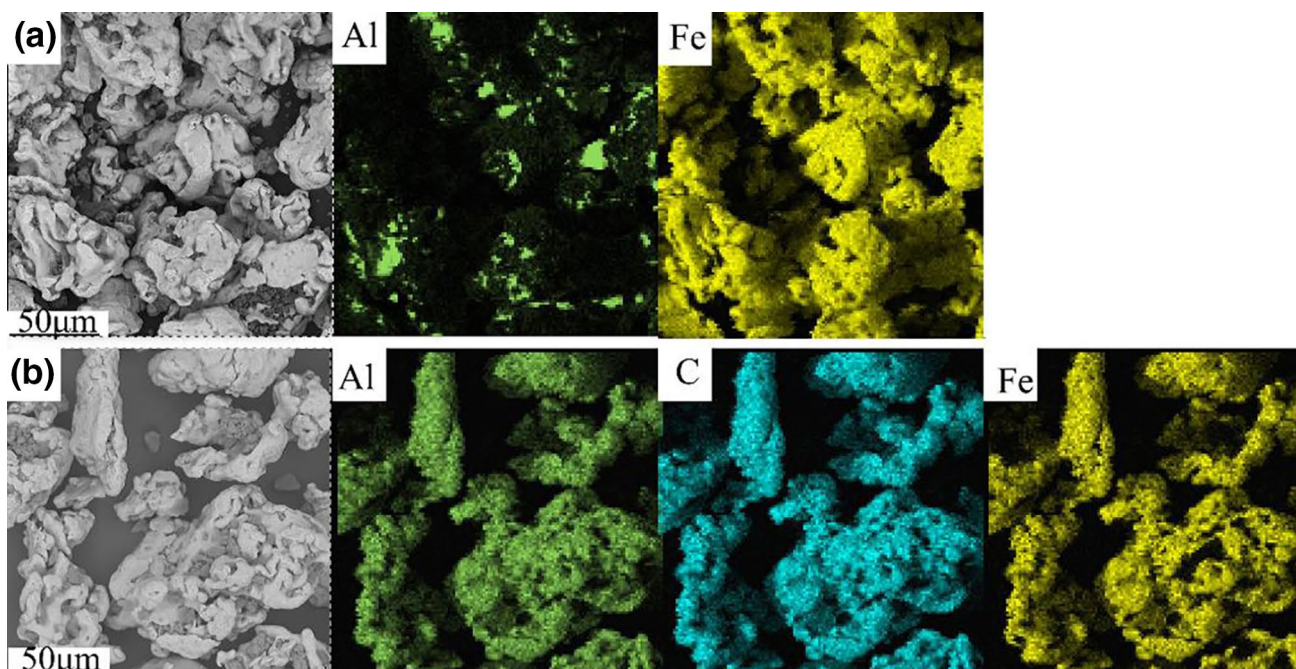
Fig. 2 Particle element distribution of magnetic powder: (a) 4% AlN-coated powder; (b) 4% AlN/phenolic resin-coated powder (Color figure online).

the composite-coated magnetic powder has abundant Al and C, indicating that the composite coating formed a continuous and dense insulation layer.

The EDS analysis of the sample coated with 4 wt.% AlN/phenolic resin is illustrated in Fig. 3, and the red arrow indicates the line sweep path. When the beam passed through the inside of the Fe particles, the elemental energy spectrum was primarily Fe, with a high peak intensity. When scanning reached the edge of the Fe powder, the peak intensity of Fe began to drop sharply, and the

peak intensity of Al and O increased, indicating that a very thin AlN layer was coated between Fe powder particles. As can be seen from the elemental distribution diagram of 4 wt.% AlN/phenolic resin-coated samples in Fig. 4, Al and O are mainly concentrated around Fe. The presence of O where Fe is present may be due to the presence of O in the phenolic resin, and the phenolic resin at the edge of Fe powder may adhere to the inside of Fe powder when polishing the sample.
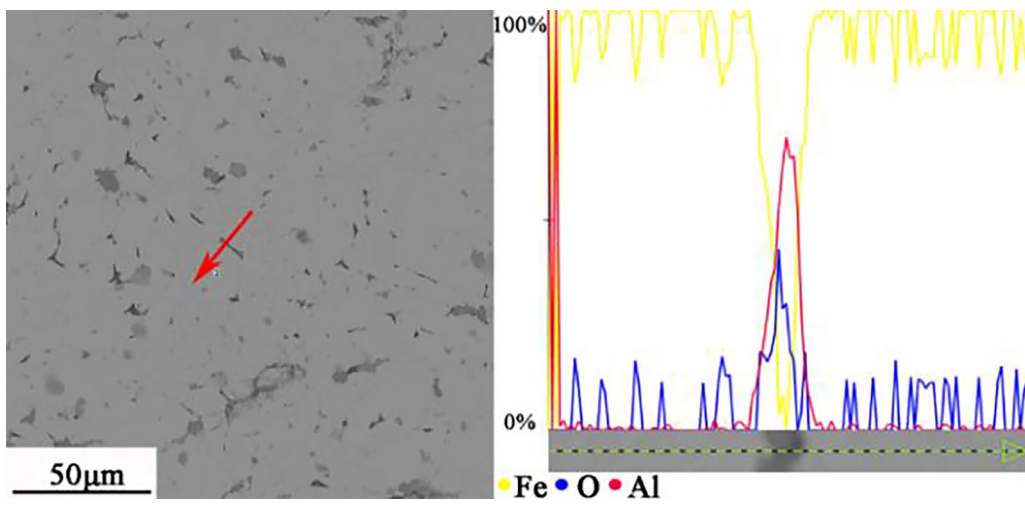
Fig. 3 Line sweep element diagram of 4% AlN/phenolic resin-coated sample (Color figure online).
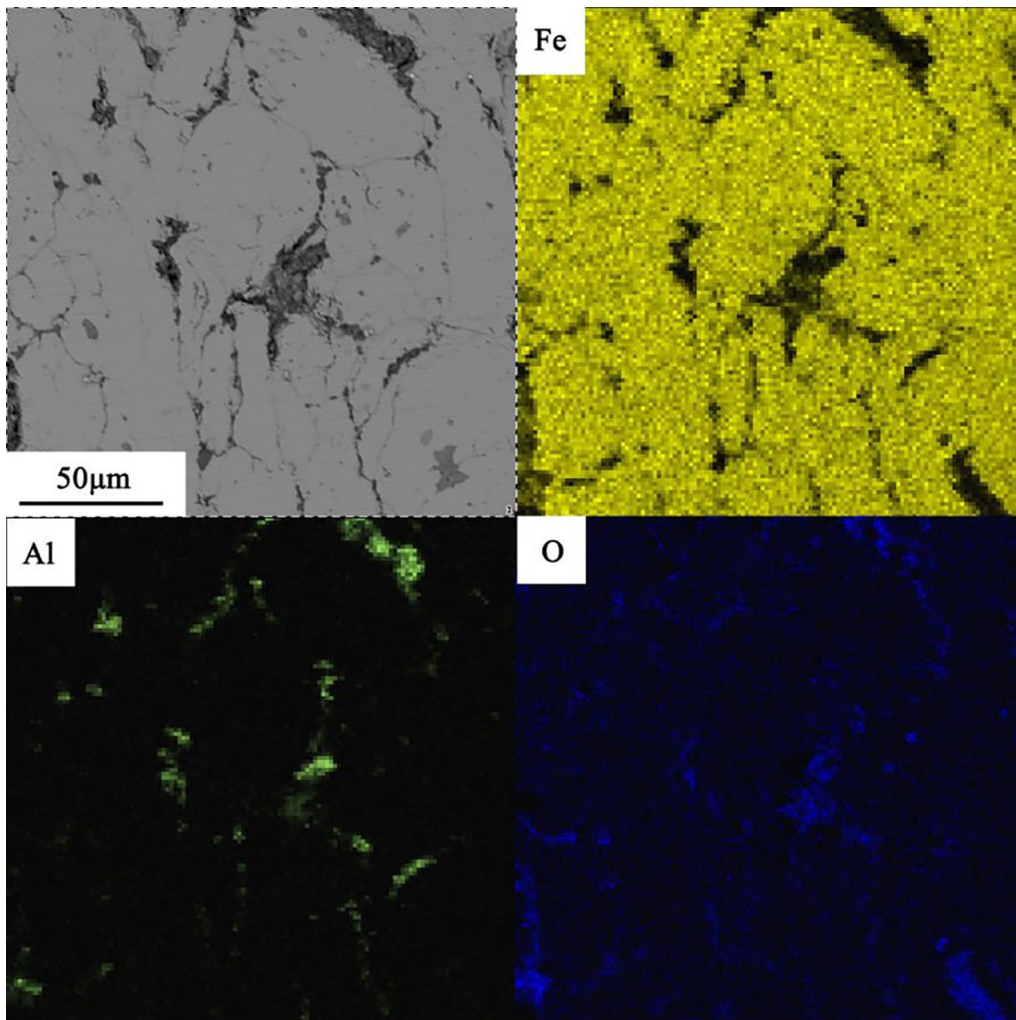

Fig. 4 Surface scanning element distribution of 4% AlN/phenolic resin-coated sample (Color figure online).

Magnetic Properties of SMCs

The magnetic loss of soft magnetic composites consists of three parts: hysteresis loss, eddy current loss and residual loss. In general, the residual loss is generated around the movement of the magnetic domain walls is usually negligible but becomes significant at very low flux densities and very high frequencies. Thus, the magnetic loss of soft magnetic composites can be expressed by the following formula.[20,21]

$$P_{CV} = P_h + P_e = f \oint H dB + \frac{C B_m^2 f^2 d^2}{\rho} \tag{1}$$

where k_2 is the proportional constant, k_2 is the frequency, k_3 is the magnetic induction intensity, d is the thickness of the material, and ρ is the resistivity of the material.

According to Eq. 1, the magnetic loss of soft magnetic composites is related to the resistivity of the specimen: the higher the resistivity, the smaller the eddy current loss, resulting in an overall reduction in total loss. In addition, magnetic loss is also related to the density of the sample, where the higher the density, the smaller the void fraction inside the sample, resulting in lower stress concentration generated at the void and smaller hysteresis loss of the sample.[22–24] The resistivity and density of different samples are summarized in Table I. The following conclusions can be drawn from the table: (1) Compared with a single inorganic AlN-coated sample, the density of the organic-inorganic composite-coated sample is relatively high. This is because it is difficult for a single AlN to completely cover the surface of the matrix, and so it is unable to fill the pores between particles, resulting in lower material density. In contrast, the organic phenolic resin in the composite coating materials has a certain fluidity and can fill in the particle gaps, effectively improving the density of the material. In the organic-inorganic composite-coated sample, the sample density decreased with the increase in AlN content, which is because the insulation coating introduces a non-magnetic phase that has lower density
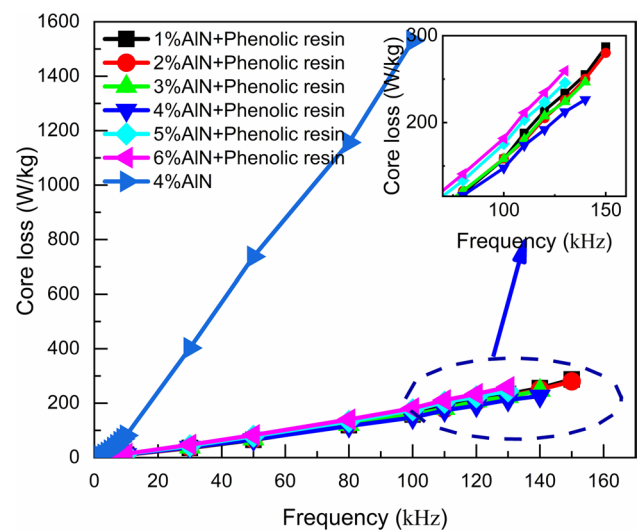
than the magnetic phase, and the increase in AlN content will lead to a decrease in the proportion of magnetic phase, resulting in a decrease in sample density. (2) The resistivity of the single AlN-coated sample was relatively low because AlN particles were not uniformly distributed on the surface of Fe particles, resulting in the generation of particle pathways. The resistivity of the sample with AlN/phenolic resin insulation was improved correspondingly, and the resistivity increased with the increase in the content of the coating agent.

Figure 5 displays the variation in the magnetic loss with frequency. The magnetic loss of the single AlN-coated specimen was large and showed a sharply increasing trend with the increase in frequency, which reached 1530.32 W/kg at 100 kHz. In contrast, the magnetic loss of the specimen coated with AlN/phenolic resin was relatively small, and the rate of increase with the increase in frequency was relatively flat, indicating that the composite coating significantly helped to reduce the magnetic loss of the sample. The magnetic loss first decreased and then increased with the increase in the coating content, which was mainly due to the addition of a certain amount of insulation coating material, which reduced the eddy current loss of the sample, thus reducing the total loss value. However, with a further increase in coating agent content, the coercive force of the material increased and the hysteresis loss increased, resulting in an increase in magnetic loss. The sample with 4 wt.% coating agent content demonstrated the lowest magnetic loss among the samples, at 147.67 W/kg under the 100 kHz test frequency.

Magnetic loss is further separated, usually expressed by the magnetic loss factor:

Table I Resistivity and density of different samples

Composition	Density (g/cm^3)	Resistivity (μΩ·m)
4% AlN	6.02	48.49
1% AlN + phenolic resin	6.95	46.15
2% AlN + phenolic resin	6.82	51.33
3% AlN + phenolic resin	6.69	52.60
4% AlN + phenolic resin	6.54	56.62
5% AlN + phenolic resin	6.46	61.28
6% AlN + phenolic resin	6.35	69.58

Fig. 5 Variation curve of magnetic loss of sample with frequency (Color figure online).

$$\tan \delta_{tot} = \frac{R_s}{2\pi fL} = \frac{R_c}{2\pi fL} + \frac{R_h}{2\pi fL} + \frac{R_e}{2\pi fL} + \frac{R_r}{2\pi fL} \qquad (2)$$

where R_s is the total loss resistance, R_c is the winding, R_h is the hysteresis loss resistance, R_e is the eddy current loss resistance, and R_r is the residual loss resistance.[25]

The loss factor of copper wire winding is as follows:

$$\tan \delta_{copper} = \frac{\rho_c l_w 10^9}{2\pi fA_w F_w F_P A_L} = \frac{k_1}{f} \qquad (3)$$

where ρ_c is the resistivity of copper coil, l_w is the length of average turns, f is the frequency, A_w is the cross-sectional area of winding, F_w is the spatial factor of copper wire winding, A_L is the inductance factor of each turn, and k_1 is the winding loss factor.[26] The hysteresis loss factor and eddy current loss factor can be expressed by the following two formulas[27]:

$$\tan \delta_h = \frac{4\upsilon B_m}{3\pi \mu_0 \mu_i^2} = k_2 \qquad (4)$$

$$\tan \delta_e = \frac{\mu_0 \mu D^2 \omega}{2\rho\beta} = \frac{\mu_0 \mu D^2 \pi f}{\rho\beta} = k_3 f \qquad (5)$$

where υ is the Ruili constant, k_2 is the hysteresis loss factor, D is the diameter of the material, ρ is the resistivity, β is the shape factor, and k_3 is the eddy current loss factor.

The residual loss and winding loss can be ignored in the application range of soft magnetic composites,[28] so the total loss factor can be expressed as follows:

$$\tan \delta_{tot} = k_2 + k_3 f \qquad (6)$$

The variation in the total loss factor with frequency is shown in Fig. 6. From Eq. 6, it can be seen that the slope in the figure represents the eddy current loss factor k_3, and the intercept of the Y-axis represents the hysteresis loss k_2. The value of k_2, k_3 can be calculated by fitting the line, and the corresponding dotted line in the figure is the fitted line. The value of k_2, k_3 under different circumstances is listed in Table II. From Fig. 6, the sample coated with the single AlN had a large slope of the fitting straight line, indicating that the eddy current loss factor was large and the insulation coating effect was not satisfactory.

As seen from Table II, the hysteresis loss factor increased with the increase in the content of the coating agent, which is because the coating material is non-magnetic and blocks the magnetic path between particles after addition. With the increase in the content of the coating, the proportion of non-magnetic phase increases, leading to the increase in the coercivity and thus the hysteresis loss of the material. The eddy current loss factor showed a decreasing trend with the increase in the coating agent content, which was because the
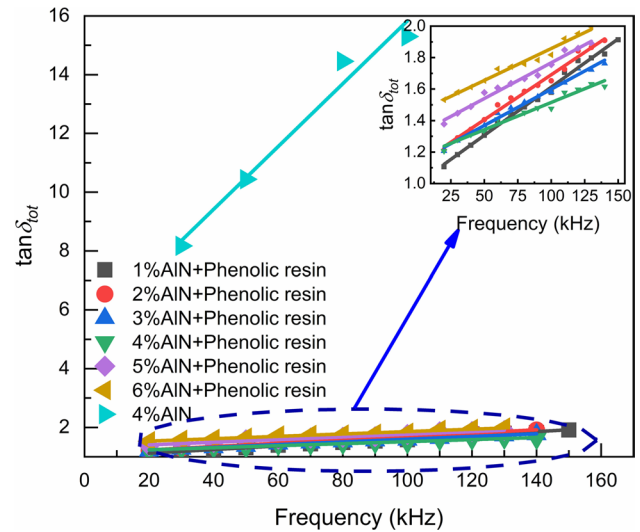

Fig. 6 The variation curve of the total loss factor of the sample with frequency (Color figure online).

Table II The hysteresis factor k_2 and eddy current loss factor k_3 of different samples

Composition	k_2	k_3
4% AlN	5.144	0.1069
1% AlN + phenolic resin	1.0004	0.0061
2% AlN + phenolic resin	1.1198	0.0057
3% AlN + phenolic resin	1.1383	0.0046
4% AlN + phenolic resin	1.1688	0.0035
5% AlN + phenolic resin	1.3126	0.0033
6% AlN + phenolic resin	1.4525	0.0032

resistivity of the sample increased with the increased coating agent content, and because the eddy current loss of the sample was inversely proportional to the resistivity, the eddy current loss factor k_3 of the sample decreased as a whole. Since the total loss of the specimen was dominated by eddy current loss at high frequencies under the applicable conditions of soft magnetic composites, the specimen had a relatively low eddy current loss factor and hysteresis loss factor when the mass fraction of the coating agent was 4 wt.%.

From the variation curve of the permeability of the sample with frequency in Fig. 7, the permeability real part of the single-coated AlN specimen decreased with the increase in frequency, indicating that the performance stability of the sample was poor. The real part of the permeability of the AlN/phenolic resin composite-coated samples tended to be stable with the increase in frequency, and the real part of the permeability gradually decreased with the increase in the coating agent content. The imaginary value of the magnetic permeability of the single-coated AlN specimen
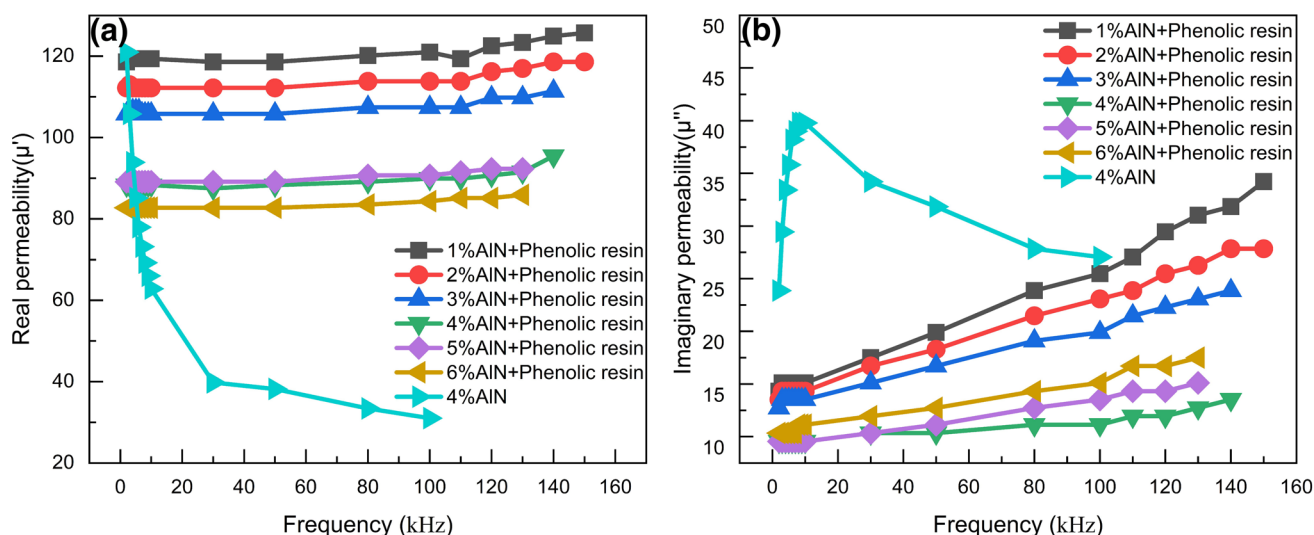
Fig. 7 Variation curve of sample permeability with frequency: (a) variation curve of sample real permeability with frequency; (b) variation curve of sample imaginary permeability with frequency (Color figure online).

peaked at about 10 kHz, indicating that the imaginary part of the single-coated AlN specimen had a cut-off frequency at this time. The magnetic permeability of the specimen using the composite coating method slowly increased with the increase in frequency, and the imaginary part of the magnetic permeability of the sample showed a trend of first decreasing and then increasing with the increase in the coating agent content, and the magnetic permeability value of the specimen was the smallest when the mass fraction of the coating agent was 4 wt.%. In summary, specimens prepared with 4 wt.% AlN/phenolic resin have the smallest imaginary value of permeability and an acceptable real value of permeability.

The quality factor is an important parameter for measuring the properties of SMCs, and the larger the quality factor, the better the material properties. The formula for calculating the quality factor of the ring sample in AC is as follows:

$$Q = \frac{\sqrt{L/C}}{R} \tag{7}$$

where L is the inductance of the AC sample, C is the capacitance of the sample, and R is the resistance value of the coil wire.[29] Figure 8 shows the variation curve of the sample quality factor with frequency. It can be seen that the quality factor of the single-coated AlN sample was relatively small on the whole, decreasing to near 1 with the increase in frequency, while the sample coated with AlN/phenolic resin showed a trend of first increasing and then decreasing with the increase in frequency. The sample quality factor was the best when the coating agent content was 4 wt.%, and the quality factor was 8.8 at 100 kHz frequency.
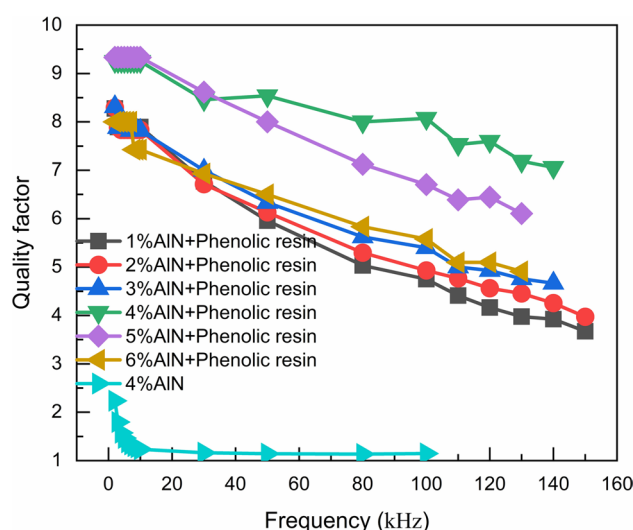
Fig. 8 Variation curve of sample quality factor with frequency (Color figure online).

Conclusion

In this work, the effects of AlN content on the microstructure, density and magnetic properties of AlN/phenolic resin-coated soft magnetic composites were examined. The results show that forming a thin and uniform AlN/phenolic resin composite insulating coating on the surface of reduced iron powder can improve the density and resistivity of the composite. The AlN/phenolic resin composite-coated sample demonstrated better magnetic properties than the single inorganic-coated sample with

AlN. At 100 kHz, the magnetic loss of the 4 wt.% AlN/phenolic resin composite-coated sample was 147.67 W/kg, which was 90.4% lower than that of the single AlN-coated sample, and the permeability was stable at 90 in a large frequency range. Based on the loss separation method, the 4 wt.% AlN/phenolic resin composite-coated sample exhibited the lowest magnetic loss and acceptable hysteresis loss factor and eddy current loss factor compared with the other samples.

Author Contributions All authors contributed to the study conception and design. Material preparation, data collection and analysis were performed by SW, ZD and JL. The first draft of the manuscript was written by ZD. The critical review and revision were carried out by YL. Supervision was conducted by JF and JL, and all authors read and approved the final manuscript.

Conflict of interest The authors declare that they have no conflict of interest.

References

1. H. Shokrollahi and K. Janghorban, Soft magnetic composite materials (SMCs). *J. Mater. Process. Technol.* 189, 1 (2007).
2. J.L. Ni, F. Hu, S.J. Feng, X.C. Han, and X.S. Liu, Soft magnetic properties of FeSiAl/carbonyl iron composites with high magnetic permeability and low magnetic loss. *J. Alloys Compd.* 887, 161337 (2021).
3. H. Song, H. Lee, J. Lee, J.K. Choe, S. Lee, J.Y. Yi, S. Park, J.W. Yoo, M.S. Kwon, and J. Kim, Reprogrammable ferromagnetic domains for reconfigurable soft magnetic actuators. *Nano Lett.* 20, 5185 (2020).
4. E.A. Perigo, B. Weidenfeller, P. Kollár, and J. Füzer, Past, present, and future of soft magnetic composites. *Appl. Phys. Rev.* 5, 031301 (2018).
5. P. Slovenský, A. Zeleáková, P. Kollár, J. Füzer, M. Jakubčin, and M. Fáberová, Preparation and characterization of fe based soft magnetic composites coated by SiO$_2$ layer prepared by Stöber method. *Acta Phy.s Pol A* 137, 872 (2020).
6. S. Wu, A.Z. Sun, Z.W. Lu, C. Cheng, and X.X. Gao, Magnetic properties of iron-based soft magnetic composites with SiO$_2$ coating obtained by reverse microemulsion method. *J. Magn. Magn. Mater.* 381, 451 (2015).
7. M. Jakubčin, Z. Birčáková, P. Kollár, R. Bures, and M. Fáberová, Study of reversible and irreversible magnetization processes proportions of Fe-MgO soft magnetic composites. *Acta Phys. Pol. A* 137, 879 (2020).
8. R. Bureš, M. Fáberová, P. Kollár, S. Dobák, F. Onderko, and P. Kurek, Microwave sintered Fe/MgO soft magnetic composite. *Acta Phys. Pol. A* 131, 780 (2017).
9. W.L. Yuan, K. Sun, J.H. Tian, Y.P. Li, Z.X. Wang, B.Y. Liu, and R.H. Fan, Improved magnetic properties of iron-based soft magnetic composites with a double phosphate-SiO$_2$ shells structure. *J. Mater. Sci. Mater. Electron.* 32, 21472 (2021).
10. Z.Q. Zhu, J.Q. Liu, H. Zhao, J. Pang, P. Wang, and J.Q. Zhang, Study of the soft magnetic properties of FeSiAl magnetic powder cores by compounding with different content of epoxy resin. *Materials* 16, 1270 (2023).
11. Z. Birčáková, J. Füzer, P. Kollár, J. Szabó, M. Jakubčin, M. Streckova, R. Bureš, and M. Fáberová, Preparation and characterization of iron-based soft magnetic composites with resin bonded nanoferrite insulation. *J. Alloys Compd.* 828, 154416 (2020).
12. S. Wu, J.C. Li, Y.J. Guan, H.K. Liu, and J.X. Liu, Research progress of preparation technology of soft magnetic composites. *J. Electron. Mater.* 41, 221 (2022). (**in Chinese**)).
13. M. Strečková, R. Bureš, M. Fáberová, Ľ Medvecký, J. Füzer, and P. Kollár, A comparison of soft magnetic composites designed from different ferromagnetic powders and phenolic resins. *Chin. J. Chem. Eng.* 23, 736 (2015).
14. M. Strečková, Ľ Medvecký, J. Füzer, P. Kollár, R. Bureš, and M. Fáberová, Design of novel soft magnetic composites based on Fe/resin modified with silica. *Mater. Lett* 101, 37 (2013).
15. S.T. Dai, T. Zhang, S.M. Mo, Y. Cai, W. Yuan, T. Ma, L. Hu, and B.Z. Wang, Study on preparation, thermal conductivity, and electrical insulation properties of epoxy/AlN. *IEEE Trans. Appl. Superconduct.* 29, 1 (2019).
16. W.W. Zhang, C. Lu, G.B. Ying, J.F. Zhang, and W. Jiang, Effect and mechanism of the surface treatment and gradation filling of AlN on the performance of insulation layer of copper clad laminate. *J. Inorg. Mater.* 36, 847 (2021).
17. H.O. Ruan, F.C. Lü, J.X. Song, X.M. Bian, K. Yin, S.D. Yin, and Q. Xie, Enhanced thermal conductance and electrical insulation of AlN/PMIA composite paper via nano splitting of matrix and size grading of fillers. *Compos. Sci. Technol.* 224, 109477 (2022).
18. B. Sinem, C. Alper, and T. Servet, Directional properties and microstructures of spark plasma sintered aluminum nitride containing graphene platelets. *J. Eur. Ceram. Soc.* 37, 3759 (2017).
19. X.X. Zhong, J.C. Chen, L. Wang, B.J. Li, and L.Z. Li, Properties of FeSiAl-based soft magnetic composites with AlN/Al2O3 and hybrid phosphate-silane insulation coatings. *J. Alloys Compd.* 735, 1603 (2018).
20. R.D. Guo, S.M. Wang, Z. Yu, K. Sun, X.N. Jiang, G.H. Wu, C.J. Wu, and Z.W. Lan, FeSiCr@NiZn SMCs with ultra-low core losses, high resistivity for high frequency applications. *J. Alloys Compd.* 830, 154736 (2020).
21. C. Xia, Y.D. Peng, X.W. Yi, Z.X. Yao, Y.Y. Zhu, and G. Hu, Improved magnetic properties of FeSiCr amorphous soft magnetic composites by adding carbonyl iron powder. *J. Non-Cryst. Solids* 559, 120673 (2021).
22. M. Anhalt, Systematic investigation of particle size dependence of magnetic properties in soft magnetic composites. *J. Magn. Magn. Mater.* 320, e366 (2008).
23. D.N. Chen, K.L. Li, H.Y. Yu, J.L. Zuo, X. Chen, B.C. Guo, G.Z. Han, and Z.W. Liu, Effects of secondary particle size distribution on the magnetic properties of carbonyl iron powder cores. *J. Magn. Magn. Mater.* 497, 166062 (2020).
24. D.H. Kim, J.G. Yeo, Y.J. Choi, S.H. Lee, S.Y. An, J.Y. Kim, and B.W. Lee, Magnetic properties of amorphous metallic composites with various particle sizes. *J. Korean Chem. Soc.* 79, 1037 (2021).
25. K. Sun, Z. Lan, Z. Yu, L. Li, X. Jiang, and H. Ji, Temperature dependence of core losses at high frequency for MnZn ferrites. *Physica B* 405, 1018e1021 (2010).
26. B. Yang, Z.B. Wu, Z.Y. Zou, and R.H. Yu, High-performance Fe/SiO$_2$ soft magnetic composites for low-loss and high-power applications. *J. Phys. D: Appl. Phys.* 43, 365003 (2010).
27. S.M. Plotnikov, Determination of eddy-current and hysteresis losses in the magnetic circuits of electrical machines. *Meas. Tech.* 63, 904 (2021).
28. G.H. Wu, Z. Yu, K. Sun, R.D. Guo, H.Y. Zhang, X.N. Jiang, C.J. Wu, and Z.W. Lan, Ultra-low core losses at high frequencies and temperatures in MnZn ferrites with nano-BaTiO$_3$ additives. *J. Alloys Compd.* 821, 153573 (2020).

29. E. Pošković, F. Franchini, and L. Ferraris, Effect of the insulating layer on the properties of SMC inductors. *Appl. Sci.* 12, 8756 (2022).

Publisher's Note Springer Nature remains neutral with regard to jurisdictional claims in published maps and institutional affiliations.